AIP | Physics of Plasmas

Extension of geodesic acoustic mode theory to helical systems

T. Watari, Y. Hamada, A. Fujisawa, K. Toi, and K. Itoh

Citation: Physics of Plasmas (1994-present) **12**, 062304 (2005); doi: 10.1063/1.1922807
View online: http://dx.doi.org/10.1063/1.1922807
View Table of Contents: http://scitation.aip.org/content/aip/journal/pop/12/6?ver=pdfcov
Published by the AIP Publishing

Extension of geodesic acoustic mode theory to helical systems

T. Watari, Y. Hamada, A. Fujisawa, K. Toi, and K. Itoh
National Institute for Fusion Science, 322-6, Oroshi-cho, Toki-city, Gifu, Japan

(Received 18 January 2005; accepted 5 April 2005; published online 26 May 2005)

The present paper extends the theory of geodesic acoustic mode (GAM) oscillation, which so far has been applied to tokamaks, to helical systems. By using drift kinetic equations for three-dimensional equilibriums, a generalized dispersion relation is obtained including Landau damping. The oscillation frequency is obtained in terms of the squared sum of Fourier components of the magnetic field intensity expressed by means of magnetic flux coordinates. An analytic form of the collisionless damping rate of GAM is obtained by solving the dispersion relation perturbatively. It is found that the GAM frequency is higher in helical systems than in tokamaks and that damping rate is enhanced in multi-helicity magnetic configurations. However, damping rates are predicted to be small if the temperature of electrons is higher than that of ions. © *2005 American Institute of Physics*. [DOI: 10.1063/1.1922807]

I. INTRODUCTION

Geodesic acoustic mode (GAM) oscillations, whose existence was reported as early as 1968,[1] are now gathering attention. Electrostatic fluctuations are divided into those with high and low mode number. Those with high mode numbers are susceptible to diamagnetic drift and are easily destabilized into drift instabilities composing the plasma turbulence. Those with low mode numbers are less susceptible to diamagnetic drift and are known to be stable; particularly, $m=0$ and $n=0$ modes are known to be long-lived having small damping rates. Among them, modes with large radial mode numbers are referred to as zonal flows, which include GAM oscillations as well as other residual flows with lower frequencies.

The interaction of the fluctuations between these two different modal ranges is broadly accepted as the key mechanisms for determining the turbulence governing the transports.[2–18] There are a number of dedicated papers in this field, which have been recently reviewed, e.g., in Refs. 11 and 12.

The existence of zonal flows including GAM has been recently demonstrated in tokamak experiments in DIII-D(Doublet-III-D)[19] by use of beam emission spectroscopy (BES), and in TEXT(Texas Experimental Tokamak),[20,21] JIPP-TII U(Japanese Institute of Plasma Physics Tokamak),[22,23] and JFT-2M(Japan Atomic Energy Research Institute Fusion Torus[24] by use of heavy ion beam probe (HIBP), respectively. Similar oscillations of potential were found also in the helical device CHS(Compact Helical System),[25] in which the mode structure has been clearly elucidated by use of a dual HIBP. In the H-1(Heliac device-1)[26] and HT-7 (Hefei Tokamak) devices,[27] where the electron temperature is low in the edge region, electrostatic probes were utilized in the experiment. Reflectometries were used in ASDEX(Axisymmetric Diverter Experiment)[28] and T-10(Tokamak-10).[29] Most significantly, these papers indicate that the associated flows are suggestive of rather narrow radial structure with the shearing rates reaching the decorrelation times. Theories suggest that GAM oscillations, as a part of zonal flow, play a role in regulating turbulences and therefore the identification of GAM and investigation of their properties are important. In order to facilitate more exact comparison of theory and experimental results, an elaboration of the GAM theories has to be made. Various sets of equations have been examined in recent theoretical studies and various expressions of GAM frequencies have appeared in the literature depending on the model adopted. Table I shows a few typical results: Refs 1 and 13–16. The three experimental papers on the other hand quoted frequencies as shown in Table II approximating the theories (Refs. 19, 22, and 25). In the experiments, they found more or less the following dependencies of the frequency on electron and ion temperatures:

$$\omega \sim \sqrt{T_e/m_i}/R \sim \sqrt{(T_e+T_i)/m_i}/R. \tag{1}$$

Though rigorous examinations in the multiplication factor remain to be made, these results are regarded as identifications of GAM. Since it often occurs in experiments that $T_e \propto T_i$ and $T_e > T_i$, the two different expressions in Eq. (1) may be practically equivalent.

The frequencies of drift wave and GAM are given, in the order estimation, by $\omega^* \sim V_T \rho_i k_y / L_n$ and $\omega \sim V_T/R$, respectively. Here V_T is the thermal velocity of ions, ρ_i is the Larmor radius of ions, L_n is the characteristic length of the plasma density, and R is the major radius. The ratio of the two frequencies $\omega/\omega^* \sim (\rho_i k_y)^{-1}(L_n/R) \sim (L_n/R)$ is not always low in the core region of the plasma. In theoretical work it is postulated that the stabilizing effect of zonal flow is weaker if its frequency is higher than the decorrelation frequency of the Drift wave turbulence.[6] Therefore, it is important to know the exact frequency of zonal flow and the mechanism of the GAM. Specifically, since GAM has been discussed based on simple tokamak configurations, it is important to examine if the same physics applies to helical systems. Since the GAM oscillation is driven by the nonlinear interaction of drift waves and is known to have resonant structure, its damping rate is important as well. If the damping is large, then the GAM oscillation will not have a large

1070-664X/2005/12(6)/062304/8/$22.50

TABLE I. The frequency of GAM oscillations suggested by theories: three typical frequencies are listed with the comments to suggest the approximation used. The damping rate is also shown where it is available.

Reference	Frequency	Damping rate	Comments
Winsor *et al.* (Ref. 1)	$\omega=\sqrt{2\gamma[(T_e+T_i)/m_i]}1/R$	Not available	Ideal MHD equation
Hallatschek *et al.* (Ref. 14)	$\omega=\sqrt{(2T_e+10/3T_i)/m_i}1/R$	Not available	Reduced from two fluid equation
Novakovskii *et al.* (Ref. 13)	$\omega=\sqrt{(7/4)(T_i/m_i)}1/R$	$\gamma_{\mathrm{GAM}}=4\nu_{ii}/7q$ collisional damping	Drift kinetic equation

enough amplitude to regulate the turbulence. Notwithstanding its importance, damping rate has not been fully investigated yet. Novakovskii gave a collisional damping rate,[13] which however may not be relevant in the hot core region. For collisionless damping, some papers suggest the following form:

$$\gamma \sim \exp(-q^2). \tag{2}$$

This expression predicts that the GAM is heavily damped in the core region of tokamaks ($q_0 \sim 1$), which may be misleading with regard to interpretation of experimental results.

The present paper attempts to reformulate the GAM oscillation by use of the drift kinetic equation and simultaneously to extend the GAM theory to helical systems. It is also shown in the process that using an appropriate GAM frequency is important in the calculation of the damping rate. In Sec. II A, a set of equations including the drift kinetic equation is presented together with approximations to be used. In Sec. II B, a general dispersion relation of the GAM oscillation is obtained including collisionless damping. In Sec. III A 1, this dispersion relation is applied to single helicity tokamak in order to show its relation to those obtained in other works. In Sec. III A 2, the general formula is applied to a straight helical system; the mechanism of GAM oscillations is made clearer through a comparison of these two simple cases. In Sec. III B, the general formula is applied to the specific CHS (Compact Helical System) configuration as an example of mixed helicity problems, where an enhancement of the damping rate is predicted.

II. DISPERSION RELATION OF GEODESIC ACOUSTIC MODE IN THREE-D CONFIGURATION

A. The equations and approximations

Winsor *et al.* predicted possible oscillation of a plasma flow by use of MHD equation.[1] In this early paper the restoring force in the GAM oscillation was shown to be radial plasma current, which is caused by the geodesic curvature of the magnetic field. This current is mostly balanced by a polarization current to satisfy quasi-neutrality. This process has a deep relationship with neoclassical theory and therefore has been studied as a transient process for reaching a neoclassical steady state.[13] Recent progress in computer simulation has been remarkable and has made it possible to simulate turbulences, including drift waves and zonal flows, globally. The presence of zonal flows is reported in most of these works. These zonal flows are naturally time-dependent, some of them showing high coherency.

The theory of GAM is generalized optimally by using the linearized drift kinetic equation:

$$\frac{\partial f_1}{\partial t} + (\boldsymbol{v}_\parallel + \boldsymbol{v}_D)\cdot\nabla f_1 + \left[\mu\frac{\partial B}{\partial t} + q(\boldsymbol{v}_\parallel + \boldsymbol{v}_D)\cdot\boldsymbol{E}\right]\frac{\partial f_0}{\partial w} = 0. \tag{3}$$

Here, $\boldsymbol{v}_\parallel$ is the velocity parallel to the magnetic field and $\boldsymbol{v}_D$ is the drift velocity of charged particles. The subscripts 0 and 1 denote the ordering according to the electric field intensity. Independent variables are kinetic energy $w=mv^2/2$ and the perpendicular magnetic invariant $\mu=mv_\perp^2/2B$. In this work, the zonal flows including GAM are assumed to be electrostatic so that

TABLE II. The frequency of GAM oscillations quoted in the experimental papers: three typical papers are listed with the differences of the experimental conditions.

Reference	Quoted frequency	Degree of agreement	Comments
JIPP T-II U (Ref. 22)	$\omega=\sqrt{T_e/m_p}1/R$	Fairly good	A tokamak with circular plasma cross section: (GAM exists wide range in plasma cross section)
DIII-D (Ref. 19)	$\omega=\sqrt{(T_e+T_i)/m_i}1/R$	Fairly good	A tokamak with single null divertor: (GAM exsists where $\rho > 0.85$)
CHS (Ref. 25)	$\omega=\sqrt{(T_e+T_i)/m_i}1/R$	Fairly good	A stellarator: (GAM measured at $\rho \sim 0.6$)

$$\mu \frac{\partial B}{\partial t} \sim 0, \quad \mathbf{E} = -\nabla \phi. \tag{4}$$

Expressing the potential ϕ as the sum of its flux surface average, $\langle \phi \rangle$, and spatial variation from it, $(\phi - \langle \phi \rangle)$, one obtains

$$\frac{\partial f_1}{\partial t} + (\boldsymbol{v}_\parallel + \boldsymbol{v}_D) \cdot \nabla f_1 + [-q(\boldsymbol{v}_\parallel + \boldsymbol{v}_D) \cdot \nabla [(\phi - \langle \phi \rangle) + \langle \phi \rangle]] \frac{\partial f_0}{\partial w} = 0. \tag{5}$$

Noting that

$$\nabla \langle \phi \rangle = \frac{\partial \langle \phi \rangle}{\partial \psi} \nabla \psi, \tag{6}$$

and assuming that $\boldsymbol{v}_D \cdot \nabla f_1$ term is smaller than $\boldsymbol{v}_\parallel \cdot \nabla f_1$ and that the $(\phi - \langle \phi \rangle)$ term is smaller than the $\langle \phi \rangle$ term, the equation reduces to the following form:

$$\frac{\partial f_{1,i}}{\partial t} + (\boldsymbol{v}_\parallel) \cdot \nabla f_{1,i} - \left[q \frac{\partial \langle \phi \rangle}{\partial \psi} (\boldsymbol{v}_D) \cdot \nabla \psi \right] \frac{\partial f_{i,0}}{\partial w} = 0, \tag{7}$$

where

$$\begin{aligned} \boldsymbol{v}_D \cdot \nabla \psi &= \frac{c}{eB^4} \frac{1}{2} \left(m v_\parallel^2 + \frac{1}{2} m v_\perp^2 \right) (\nabla \psi \times \boldsymbol{B}) \cdot \nabla B^2 \\ &= \frac{c}{eB^2} \left(m v_\parallel^2 + \frac{1}{2} m v_\perp^2 \right) |(\nabla \psi \times \boldsymbol{B})| \kappa_g. \end{aligned} \tag{8}$$

The third term in Eq. (7) has the geodesic curvature κ_g, manifesting itself as the cause driving radial current and serving the GAM oscillations restoring force.

The electron version of Eq. (3) has the following simpler form if the inertial term is ignored:

$$(\boldsymbol{v}_\parallel + \boldsymbol{v}_D) \cdot \nabla f_{1,e} + \frac{-1}{T_e} [-q_e (v_\parallel + v_D) \cdot \nabla (\phi - \langle \phi \rangle)] f_{e,0} = 0. \tag{9}$$

The solution to Eq. (9) is easily found to be

$$f_{1,e} = -\frac{q_e}{T} [(\phi - \langle \phi \rangle)] f_{e,0}. \tag{10}$$

In the following analysis we assume charge neutrality $q_e n + q_i n_i = 0$ to obtain the electron distribution function

$$f_{1,e} = -\frac{q_e}{T_e} [(\phi - \langle \phi \rangle)] f_{e,0} = -\frac{q_i}{q_e} \left(\int f_i d\boldsymbol{v} \right) (f_{e,0}/n_{e,0}). \tag{11}$$

Therefore, in this procedure of calculation, the variation of the potential within the flux surface does not play a role but is associated with the ion distribution.

$$[(\phi - \langle \phi \rangle)] = T_e \frac{q_i}{q_e^2} \left(\int f_{1,i} d\boldsymbol{v} / n_{e,0} \right). \tag{12}$$

B. Ion and electron distribution functions

By using a magnetic flux coordinate and adopting co- and contra-variant expressions, the magnetic field intensity is Fourier decomposed in the following form:

$$B^2 = \sum_{m,n} B_0^2 (1 + \delta_{m,n} \cos(m\theta - n\zeta)). \tag{13}$$

Here, θ and ζ are the poloidal and toroidal like angles. Correspondingly, $f_{1,i}$ is expanded in a Fourier series as

$$f_{1,i} = \sum_{m,n} (f_s(m,n) \sin(m\theta - n\zeta) + f_c(m,n) \cos(m\theta - n\zeta)). \tag{14}$$

Equation (7) then assumes the form:

$$\begin{aligned} \frac{\partial f_s}{\partial t} &- \frac{1}{B} (m B^\theta - n B^\zeta) v_\parallel f_c \\ &= ec \frac{\partial \phi}{\partial \psi} \left(\frac{(m v_\parallel^2 + \frac{1}{2} m v_\perp^2)}{2T} \right) \frac{1}{\sqrt{g} B^2} (m B_\zeta + n B_\theta) \delta_{m,n}(\psi) f_0, \\ \frac{\partial f_c}{\partial t} &+ \frac{1}{B} (m B^\theta - n B^\zeta) v_\parallel f_s = 0. \end{aligned} \tag{15}$$

In deriving Eq. (15), $(v_\parallel, v_\perp)$ were chosen as independent variables in place of (w, μ), and the following term of the order $\delta_{m,n}$ has been ignored:

$$-(\boldsymbol{v}_\parallel + \boldsymbol{v}_d) \cdot \left(\frac{1}{2} \left(\frac{1}{m v_\parallel} B \right) m \frac{(v^2 - v_\parallel^2)}{B^2} \nabla B \right) \frac{\partial f}{\partial v_\parallel}. \tag{16}$$

The solution to Eq. (14) has the form

$$\begin{aligned} f_s = &\frac{(-i\omega)}{-(\omega - k_\parallel v_\parallel)(\omega + k_\parallel v_\parallel)} \\ &\times ec \frac{\partial \phi}{\partial \psi} \left(\frac{(m v_\parallel^2 + \frac{1}{2} m v_\perp^2)}{2T} \right) \frac{1}{\sqrt{g} B^2} (m B_\zeta \\ &+ n B_\theta) \delta_{m,n}(\psi) f_0, \end{aligned} \tag{17}$$

$$f_c = \frac{1}{i\omega} (m B^\theta - n B^\zeta) \frac{1}{B} v_\parallel f_s \tag{18}$$

with

$$k_{\parallel,m,n} = \frac{1}{B} (m B^\theta - n B^\zeta). \tag{19}$$

In the following calculation, we need only f_s, while f_c gives the plasma flow within the flux surface. In this paper, ψ, Φ, and $\sqrt{g}$ are poloidal flux, toroidal flux, and Jacobian, respectively. Since $B^\theta \propto B^\zeta \propto 1/\sqrt{g}$, in coordinates of straight magnetic field lines, the other freedom could be used so that $\sqrt{g} \propto 1/B$ in order to make $k_\parallel$ independent of (θ, ζ). However, within the scope of this paper, where the distribution function is solved in first order in $\delta_{m,n}$, the choice of the coordinate system is not important. If $k_\parallel$ is dependent on (θ, ζ), it may be replaced by its mean value. A Boozer coordinate can be used as well, a merit of which is that $(m B_\zeta + n B_\theta)$ is independent of (θ, ζ) and does not create a further family of harmonics on the right-hand side of Eq. (15). From the same point of view, a straight magnetic-field-line coordinate is not a requirement either.

Equation (14) suggests that GAM is characterized only by the parameters $\delta_{m,n}$ and that therefore the prediction of GAM may be dependent on the choice of the coordinate system. This apparent paradox may be possibly reconciled by the interpretation that that the sum of the contributions from all the Fourier components gives approximately the same result.

C. The dispersion relation of GAM oscillation

The current due to the geodesic curvature $\boldsymbol{j}_\kappa$ is expressed by use of the distribution function

$$\boldsymbol{j}_\kappa = \sum_{i,e} q \int (\boldsymbol{v}_D f_1) d\boldsymbol{v}. \tag{20}$$

The dispersion relation is obtained by balancing the current $\boldsymbol{j}_\kappa$ with the polarization current, $\boldsymbol{j}_p$:

$$\int \boldsymbol{j}_\perp \cdot d\boldsymbol{S} = \int \sqrt{g}(\boldsymbol{j}_\kappa + \boldsymbol{j}_p) \cdot \boldsymbol{\nabla} \psi d\theta d\zeta = 0. \tag{21}$$

For the ion contribution of the current due to the geodesic curvature, we obtain

$$\int \sqrt{g}\left(q_i\left(\int (\boldsymbol{v}_{D,i}) \cdot \boldsymbol{\nabla} \psi\right) f_{1,i} d\boldsymbol{v}\right) d\theta d\zeta \sim -\frac{e^2c^2}{2} n_{0,i} T_i \frac{\partial \phi}{\partial \psi}\left(\frac{1}{\sqrt{g}B^2}\right)^2 (mB_\zeta + nB_\theta)^2 \delta^2_{m,n}(\psi)\left(\frac{1}{2}\tilde{V}'\right) \times F_{i,m,n}. \tag{22}$$

Here,

$$F_{i,m,n} = F_i(\zeta_{m,n}) \equiv \int \left(\frac{1}{i(\omega - k_{\parallel,m,n} v_\parallel)} + \frac{1}{i(\omega + k_{\parallel,m,n} v_\parallel)}\right) \times \left(\frac{\left(m_i v_\parallel^2 + \frac{1}{2} m_i v_\perp^2\right)}{2T_i}\right)^2 f_{i,0} d\boldsymbol{v} \tag{23}$$

with

$$\zeta_{m,n} = \frac{\omega}{k_{\parallel,m,n} v_{T,i}}. \tag{24}$$

$\tilde{V}'$ is defined as follows and approximated:

$$\left(\frac{1}{2}\tilde{V}'\right) \equiv \int \sin^2(m\theta - n\zeta)\sqrt{g} d\theta d\zeta \sim \left(\frac{1}{2}V'\right). \tag{25}$$

In obtaining Eq. (22) and in the following calculation, the integration over $(v_\parallel, v_\perp)$ is made before the integration over (θ, ζ). Quantities weakly dependent on (θ, ζ) are then put out of the integration and replaced with their mean values without individual mention.

The electron contribution is similarly calculated substituting Eq. (11) into Eq. (18). This process may be equivalent to adopting an adiabatic electron response and therefore the electron contribution to the dissipative part of the response is small.

Adding the contributions both from ions and electrons we obtain

$$F_{m,n} = F_{i,m,n} + F_{e,m,n} = 2\frac{-i}{\omega}\frac{1}{T_i}\left(T_e + \frac{7}{4}T_i\right)\left[1 + \xi \cdot \left(\frac{k^2_{\parallel,m,n} v^2_{T,i}}{\omega^2}\right)\right] + \frac{2\sqrt{\pi}}{\omega}\zeta_{m,n}\left(\zeta^4_{m,n} + \zeta^2_{m,n} + \frac{1}{2}\right)\exp(-\zeta^2_{m,n}) \tag{26}$$

with

$$\xi \equiv \frac{(T_e + (23/8)T_i)}{(T_e + (7/4)T_i)} \sim 1. \tag{27}$$

Substituting the expression of polarization current

$$\boldsymbol{j}_p = \frac{\omega^2_{p,i}}{\omega^2_{c,i}} \frac{\omega}{4\pi i} \frac{d\phi}{d\psi} \boldsymbol{\nabla} \psi \tag{28}$$

into Eq. (18), the divergence of the polarization current is obtained in the following form:

$$\int \boldsymbol{j}_p \cdot d\boldsymbol{S} = \frac{\omega}{4\pi i}\frac{d\phi}{d\psi}\int \frac{\omega^2_{p,i}}{\omega^2_{c,i}}\sqrt{g}|\nabla \psi|^2 d\theta d\zeta \approx \frac{\omega^2_{p,i}}{\omega^2_{c,i}}\frac{\omega}{4\pi i}\frac{d\phi}{d\psi}\frac{qB_\zeta + B_\theta}{2\pi}\int \frac{1}{B^2}|\boldsymbol{\nabla} \psi|^2 d\theta d\zeta. \tag{29}$$

Defining

$$\tilde{\omega}^2_{G,m,n} \equiv \frac{\frac{e^2c^2}{2} n_{0,i} T_i \left(\frac{1}{\sqrt{g}B^2}\right)^2 (mB_\zeta + nB_\theta)^2 \delta^2_{m,n}(\psi)\left(\frac{1}{2}\tilde{V}'\right)}{\frac{\omega^2_{p,i}}{\omega^2_{c,i}}\frac{1}{4\pi}\frac{qB_\zeta + B_\theta}{2\pi}\int \frac{1}{B^2}|\boldsymbol{\nabla} \psi^2| d\theta d\zeta} \tag{30}$$

the dispersion relation is cast in a simple form

$$\omega^4 - \omega^2 \sum_{m,n} \omega^2_{G,m,n} F_{m,n} = 0. \tag{31}$$

That is,

$$\omega^4 - 2\left(T_e + \frac{7}{4}T_i\right)\sum_{m,n}\frac{1}{T_i}\tilde{\omega}^2_{G,m,n}[(\omega^2 + \xi k^2_{\parallel,m,n} v^2_{T,i})] = \sum_{m,n} -i2\sqrt{\pi}\omega^2_{G,m,n}\omega^2 \zeta_{m,n}\left(\zeta_{m,n}{}^4 + \zeta_{m,n}{}^2 + \frac{1}{2}\right) \times \exp(-\zeta_{m,n}{}^2). \tag{32}$$

The solution to (32) is easily obtained if the imaginary part is assumed small compared to the real part:

$$\mathrm{Re}\ \omega^2 = \sum_{m,n} 2\left(T_e + \frac{7}{4}T_i\right)\frac{1}{T_i}\tilde{\omega}^2_{G,m,n} + \frac{\xi}{\sum_{m,n}\tilde{\omega}^2_{G,m,n}}\left(\sum \tilde{\omega}^2_{G,m,n}(k^2_{\parallel,m,n} v^2_{T,i})\right), \tag{33}$$

$$\gamma = -\operatorname{Im}\omega = -(2\omega)^{-1}\sqrt{\pi}\sum_{m,n}\omega_{G,m,n}^2\zeta_{m,n}\left({\zeta_{m,n}}^4 + {\zeta_{m,n}}^2 + \frac{1}{2}\right)\exp(-{\zeta_{m,n}}^2). \tag{34}$$

The following identities and approximations are used further to simplify Eq. (33):

$$V' \equiv \frac{dV}{d\psi} = \frac{d\Phi}{d\psi}\frac{dV}{d\Phi} \sim \frac{(2\pi)qR}{B_t},$$

$$\sqrt{g}B^2 = (qB_\zeta + B_\theta)/2\pi, \tag{35}$$

$$qB_\zeta + B_\theta \sim qRB_t, \quad mB_\zeta + nB_\theta \sim mRB_t.$$

Here, q is the safety factor and V' is the specific volume. We define

$$l_\psi^2 \equiv \frac{q^2}{(2\pi)^2}\int \frac{1}{B^2}|\nabla\psi^2| d\theta d\zeta \tag{36}$$

as an index to the radial wave number. Occasionally, for easy calculation, it is regarded as the circumferential length of the poloidal cross section of a flux surface.

Using the above approximations, the following simplification is made with fairly good accuracy:

$$\tilde{\omega}_G^2 = \left[\frac{T_i}{m}\right]\frac{1}{R^2}\cdot\left(\frac{mB_\zeta + nB_\theta}{RB_t}\right)^2\frac{\delta^2{}_{m,n}(\psi)}{4(l_\psi/2\pi R)^2}$$
$$\sim \left[\frac{T_i}{m}\right]\frac{1}{R^2}\cdot\sum_{m,n}\frac{m^2\delta^2{}_{m,n}(\psi)}{4(l_\psi/2\pi R)^2}. \tag{37}$$

III. APPLICATIONS OF THE FORMULA TO SPECIFIC PROBLEMS

A. Single helicity plasma

1. Application to a tokamak of circular plasma cross section

For instance, the JIPP T-IIU tokamak has circular flux surfaces in low beta operations and belongs to the class of single helicity tokamaks.[22] Thus the magnetic field has a single dominant Fourier component, i.e., toroidal ripple

$$\delta_{m=1,n=0}(\psi) \sim (2\varepsilon) = 2(r/R). \tag{38}$$

The factor of 2 comes from the fact that B^2 is Fourier analyzed instead of B as defined in Eq. (11). The coordinate system used here is the "natural" coordinate defined by $dl^2 = (2\pi RB_p)^{-2}d\psi^2 + r^2 d\theta^2 + R^2 d\zeta^2$. The Jacobian is then $\sqrt{g} = 2\pi r(1/B_p) \propto 1/B$, though the magnetic field is not straight. By using Eq. (37) and assuming $l_\psi/2\pi = r$, Eq. (37) reduces to the popular form characterizing GAM,

$$\tilde{\omega}_G^2 = \left[\frac{T_i}{m}\right]\frac{1}{R^2}, \tag{39}$$

and Eq. (29) reduces to

$$\operatorname{Re}\omega^2 = 2\left(T_e + \frac{7}{4}T_i\right)\frac{1}{m_i}\frac{1}{R^2} + \xi(k_{\parallel,m=1,n=0}^2 v_{T,i}^2) \tag{40}$$

with

$$k_{\parallel,m=1,n=0} = \frac{1}{B_0}(B^\theta) \sim \frac{1}{qR}. \tag{41}$$

The GAM frequency Eq. (40) is different from those referred to in Table I in some details: The numerical factor γ in Ref. 1 is explicitly given in Eq. (40) giving different values for electrons and ions. It agrees with Ref. 14 and disagrees with others in the factor multiplied to T_e. This is attributed to the fact that adiabatic approximation was used for electrons in this paper and in Ref. 14. It agrees with Ref. 13 in the multiplication factor to T_i and disagrees with the others, for the drift kinetic equation was used in the two papers. The second term in Eq. (40) was not given regard in Refs. 13 and 14, which however may be important for an accurate determination of the damping rate.

The damping rate is easily obtained from Eq. (35) as

$$\gamma = -\operatorname{Im}\omega = -(2)^{-1}\left(2\left(\tau^{-1} + \frac{7}{4}\right)\right)^{-1/2}$$
$$\times\sqrt{\pi}\omega_{G,m=1,n=0}\zeta_{m=1,n=0}\left({\zeta_{m=1,n=0}}^4 + {\zeta_{m=1,n=0}}^2 + \frac{1}{2}\right)$$
$$\times\exp(-{\zeta_{m=1,n=0}}^2) \tag{42}$$

with

$$\tau = T_i/T_e. \tag{43}$$

In this expression, we find the multiplication factor to the exponent is not as simple as that referred to in the literature. However, we still consider it less important than the matching parameter on the shoulder of the exponent,

$$\gamma \propto \exp(-{\zeta_{m=1,n=0}}^2) = \exp\left(-\frac{\omega^2}{k_{\parallel,m=1,n=0}^2 v_{T,i}^2}\right)$$
$$= -\exp\left(-\left(\tau^{-1} + \frac{7}{4}\right)q^2 - \xi\right)$$
$$= -\exp\left(-\left(\tau^{-1} + \frac{3}{4}\right)q^2 - \xi\right)\exp(-q^2). \tag{44}$$

The last transformation enables a comparison with Eq. (2). Equation (44) gives a much smaller damping rate than is estimated using Eq. (2) due to the larger value in the exponent in front. Particularly, it is noted that the damping is weak if the electron temperature is higher than that of ions.

2. Application to a straight helical system

For a straight helical system with single helicity $(m,n) = (M,N)$, the following results are obtained through similar calculations:

$$\operatorname{Re}\omega^2 = 2\left(T_e + \frac{7}{4}T_i\right)\frac{1}{m_i}\frac{1}{R^2}M^2\frac{\delta_{M,N}^2}{4(l_\psi/2\pi R)^2} + \xi\cdot(k_{\parallel,M,N}^2 v_{T,i}^2), \tag{45}$$

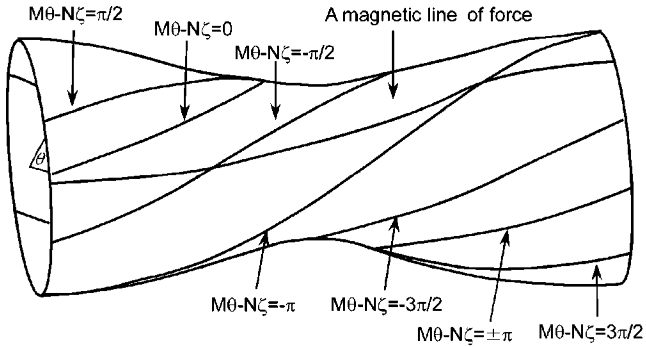

FIG. 1. Illustration of a single helicity helical system, which is most easily realized as a straight helical system. A flux surface is shown for a supposed $M=2$, $N=10$ helical system for one toroidal pitch $(0<\zeta<2\pi/N)$. The pressure increment and decrement occur along the lines $M\theta-N\zeta=2l\pi\pm\pi/2$, where the geodesic curvature is large. It is also seen that the connection length is short in a helical system.

$$\mathrm{Im}\,\omega=-(2)^{-1}\left(2\left(\tau^{-1}+\frac{7}{4}\right)\right)^{-1/2}\sqrt{\pi}\tilde{\omega}_{G,M,N}\zeta_{M,N}\left({\zeta_{M,N}}^4+{\zeta_{M,N}}^2+\frac{1}{2}\right)\exp(-{\zeta_{M,N}}^2) \tag{46}$$

with

$$k_{\parallel,M,N}=\frac{1}{B_0}(MB^\theta-NB^\zeta). \tag{47}$$

The parameter on the shoulder of the exponent ${\zeta_{M,N}}^2$ has an important role in determining the intensity of the damping; if it is reduced to close to unity the damping becomes substantial. Since this parameter is the wave phase velocity relative to the thermal speed of ions, it may be called the matching parameter. The matching parameter is transformed as

$$\begin{aligned}{\zeta_{M,N}}^2&=\frac{\omega^2}{k_{\parallel,M,N}^2v_{T,i}^2}=\left(\tau^{-1}+\frac{7}{4}\right)\frac{B_0^2}{(MB^\theta-NB^\zeta)^2R^2}+\xi\\&\sim\left(\tau^{-1}+\frac{7}{4}\right)\frac{1}{N^2}\frac{q^2}{((M/N)-q)^2}+\xi.\end{aligned} \tag{48}$$

It is found that, the damping of GAM is stronger in helical systems than in tokamaks due to the factor $(1/N)^2$. This is due to the fact that positive and negative geodesic curvature appears in toroidal pitch N as illustrated in Fig. 1. The accumulations of ions and electrons occur in a helical system along the line of $M\theta-N\zeta=2l\pi\pm\pi/2$, while it occurs in tokamaks along the line of $\theta=\pm\pi/2$. Since the magnetic field is mostly in the toroidal direction, the connection length, i.e., the inverse of the wave number, scales as $1/N$. At first observation, this factor is large making damping stronger. One interesting feature is however that the matching parameter becomes large around the resonance surface, where $(1-(M/N)q(\psi))\sim 0$. Such a resonance surface appears at around the last closed flux surface where separatrix and diverter exist. It is noted however that this method may not be very accurate near the separatrix due to the adopted formal expansion with respect to $\delta_{m,n}$. Also, ion orbit losses have to be taken into consideration in order to associate the predictions with H modes, an interesting phenomenon of the diverted edge plasma.

B. Mixed helicity systems (application to the Compact Helical System CHS)

Since a general formula was given by Eqs. (33) and (34), it is simply applied to specific configurations. The magnetic field in CHS is approximated as

$$B\approx B_0(1-0.15\rho\cos\theta+0.25\rho^2\cos(2\theta-8\zeta)+\cdots) \tag{49}$$

with two dominant Fourier components: helical ripple $\delta_{m=2,n=8}\approx 0.5\rho^2$ and toroidal ripple $\delta_{m=1,n=0}\approx 0.3\rho$. Here, the minor radius index ρ is defined in terms of toroidal flux Φ as $\rho\equiv\sqrt{\Phi/\Phi_{\mathrm{LCFS}}}$. The frequency of the GAM is then easily obtained from (34),

$$\begin{aligned}\mathrm{Re}\,\omega^2&=2\left(T_e+\frac{7}{4}T_i\right)\frac{1}{m_i}\frac{1}{R^2}\left(1+2^2\left(\frac{\delta_{m=2,n=8}}{\delta_{m=1,n=0}}\right)^2\right)\\&\quad\times\left(\frac{\delta_{m=1,n=0}/2}{l_\psi/2\pi R}\right)^2\\&\quad+\xi\frac{1}{\sum_{m,n}\tilde{\omega}_{m,n}^2}\{\tilde{\omega}_{m=2,n=8}^2(k_{\parallel,m=2,n=8}^2v_{T,i}^2)\\&\quad+\tilde{\omega}_{m=1,n=0}^2(k_{\parallel,m=1,n=0}^2v_{T,i}^2)\}.\end{aligned} \tag{50}$$

Around $\rho\sim 0.6$ where measurements were made,[25] the two ripples have similar sizes and the helical ripple gives a larger contribution due to the factor 2^2. By using CHS parameters $R=92$ cm and $l_\psi\sim 75$ cm we have

$$\left(1+2^2\left(\frac{\delta_{m=2,n=8}}{\delta_{m=1,n=0}}\right)^2\right)\sim 5,\quad\left(\frac{\delta_{m=1,n=0}/2}{(l_\psi/2\pi R)}\right)^2\sim 0.47. \tag{51}$$

Thus the GAM oscillation in CHS is estimated to be 1.5 times as high as it would be in a tokamak of circular plasma cross section. Though the mechanism is quite different, the GAM frequency is not much different numerically from that expected for a tokamak of similar size.

For the damping rate, only the helical contribution, i.e., $(m,n)=(2,8)$ may be kept:

$$\begin{aligned}\gamma&=-\mathrm{Im}\,\omega=-(2)^{-1}\left(2\left(\tau^{-1}+\frac{7}{4}\right)\right)^{-1/2}\left(1+2^2\left(\frac{\delta_{m=2,n=8}}{\delta_{m=1,n=0}}\right)^2\right)^{-1/2}\left(\frac{\delta_{m=1,n=0}/2}{(l_\psi/2\pi R)}\right)^{-1/2}\\&\quad\times\sqrt{\pi}\tilde{\omega}_{G,m=2,n=8}^2\zeta_{m=2,n=8}\left({\zeta_{m=2,n=8}}^4+{\zeta_{m=2,n=8}}^2+\frac{1}{2}\right)\exp(-{\zeta_{m=2,n=8}}^2),\end{aligned} \tag{52}$$

$$k_{\parallel,2,8}=\frac{1}{B_0}(2B^\theta-8B^\zeta). \tag{53}$$

The matching parameter is written as

$$\zeta_{m=2,n=8}{}^2 \sim \left(\tau^{-1} + \frac{7}{4}\right)\frac{1}{8^2}\frac{q^2}{(q-(2/8))^2} + \xi. \tag{54}$$

In this example, substituting $q \sim 2$, $\tau^{-1} \sim 10$, $\xi \sim 1$, we obtain

$$\zeta_{m=2,n=8}{}^2 \sim 1.$$

Thus it is supposed that GAM oscillation may be small in amplitude, for the damping is substantial. The equilibrium used in this section was obtained by use of VIEMEC code and (θ,ζ) are those of the VIEMEC coordinate. It gives a narrow spectrum dominated by two components: helical and toroidal ripples.

IV. DISCUSSION

It is interesting to review the obtained formula and its applications to specific problems. Equation (2) suggests that GAM oscillations may be heavily damped in the core of tokamaks where the q value is small. Indeed, Ref. 19 reports that the GAM oscillation was found only near the edge where q is large. In JIPPT-IIU data however, the GAM oscillation was found instead in the core region with a larger amplitude and high coherency. The newly obtained formula shows that the damping rate is much smaller by the extra factors included in Eq. (44). Particularly, our new expression suggests that the damping rate could be effectively smaller if the electron temperature is large compared to ion temperature. In the JIPP-T-II U device, a low density Ohmic plasma was used where $Te > 3Ti$ and thus the damping rate is estimated to be very small.[22] This feature resembles to that of the ion acoustic mode, where frequency is determined by electron temperature and therefore the phase velocity of the wave can be higher than the thermal speed of ions. The GAM was found only in the region $\rho > 0.85$ in the DIII-D experiment.[19] This result may also be explained by the present model, if NBI was used in the DIII-D experiment so that $Te \sim Ti$.

As to helical systems, it has to be kept in mind that q is larger toward the center of the plasma. Applied to the experiment in CHS, the formula derived here suggests an even stronger enhancement of the damping rate due to the factor $(1/N)^2$. The new expression suggests also that the connection length becomes numerically large toward the edge of the plasma and that the damping is reduced. Such mechanism is not substantial in CHS but may be operative in LHD (Large Helical Device in National Institute for Fusion Science) for it has a separatrix. The electron temperature in CHS may be ten times larger than ion temperature.[25] These effects may combine to mitigate the strong damping rate of GAM oscillation. [It is noted however in the core region (say, $\rho < 0.4$) ripple is dominated by toroidal ripple and the nature of the GAM may approach that of tokamaks. Since the safety factor increases toward the center of the plasma conversely to tokamaks, there is another chance of mitigation of damping.]

The formula obtained here is in principle applicable to other classes of devices including multi-helicity: quasi-toroidal, quasi-helical, and iso-dynamical configurations. In some of these cases, full integration may have to be made instead of using approximations (35) and (36) below. Noncircular tokamaks also belong to this class with B having $(m=2, n=0)$ and $(m=3, n=0)$ components corresponding to ellipticity and triangularity. Thus, the present formula suggests an enhancement of damping for them.

We recall a tendency in tokamak experiments for the energy confinement time to be degraded into L-mode scaling as soon as additional heating is applied to Ohmic plasma. A possible conjecture is that GAM is playing some roles in regulating turbulence in the Ohmic plasma, but not in the additional heating phase where Ti tends to approach Te. In this paper, GAM oscillation was investigated under the formal ordering where GAM oscillation is obtained to the order $\delta^2_{m,n}$. While this formalism allows us direct comparison to the results of work done in the past, it fails to incorporate the role of trapped ions, newly recognized through this work. They may play an important role in the low frequency range. The present paper limits its scope to high-frequency zonal flows by using asymptotic expansions and stays consistent to the adopted approximation. The low frequency range will be investigated in a more general way and results will be published as a separate paper.

V. CONCLUSIONS

In this paper the theory of GAM was extended to helical systems. The GAM oscillation relies for its restoring force on the geodesic curvature, which is given as a scalar function over (θ,ζ). Since the GAM oscillation is characterized by $m=0$ and $n=0$, the overall restoring force is just the square integral of the geodesic curvature over θ and ζ. The extension to helical system may be rather easy after this insight is reached. The obtained GAM frequency is written in terms of the squared Fourier component of the magnetic field intensity. This form suggests that Parseval's theorems apply. The GAM frequency in a helical system may be higher than that in a tokamak of similar major radius, for the former relies for its rotational transform necessarily on the higher harmonic numbers, which are accompanied by larger curvature of the magnetic lines of force. It is also found that the damping is stronger in helical systems than in tokamaks due to the shorter connection length associated with the larger toroidal mode number. The connection length, however, becomes large in the radial domain satisfying $m-nq=0$ and damping is suggested to be weak. In CHS, this layer is outside the plasma and therefore mitigation of damping by this mechanism may be small. On the other hand, Te/Ti is high in CHS and supposed to mitigate the damping to a certain level. However, the damping is still substantial accounting for the fact that the GAM oscillation is smaller in amplitude than the residual zonal flows in the lower frequency and smaller than the GAM observed in JIPP T-IIU. The same formula is applied to tokamaks of noncircular cross section, regarding them as presenting a type of multi-helicity problem. Here, it also suggests an enhancement of the damping rate due to the presence of the harmonics with their shorter connection length.

In all the cases considered, the damping rate is small for large values of Te/Ti. Comparison of the experimental transport coefficients with the damping rate of the GAM in their radial structure and dependence on Te/Ti may give some clues to an assessment of the role of GAM with its shearing rate in regulating turbulences.

ACKNOWLEDGMENTS

The authors acknowledge useful discussions with Dr. M. Isobe at NIFS, Dr. Y. Zhao at ASIPP, Dr. J.Dong at SWIP.

This work is partly supported by JSPS-CAS Core University Program in the field of [plasma and nuclear fusion] as well as JSPS Grant-in-Aid for Scientific Research [15206107]. The author thanks Dr. T. Notake for preparation of the illustration (Fig. 1).

[1] N. Winsor, J. L. Johnson, and J. M. Dawson, Phys. Fluids **11**, 2448 (1968).
[2] A. Hasegawa and M. Mima, Phys. Fluids **21**, 87 (1978).
[3] A. Hasegawa and M. Wakatani, Phys. Rev. Lett. **59**, 1581 (1987).
[4] P. H. Diamond, S. Champeaux, M. Malkov *et al.*, Nucl. Fusion **41**, 1067 (2001).
[5] K. Itoh and S-I. Itoh., Plasma Phys. Controlled Fusion **38**, 1 (1996).
[6] T. S. Hahm, M. A. Beer, Z. Lin, G. W. Hammett, W. W. Lee, and W. M. Tang, Phys. Plasmas **6**, 922 (1999).
[7] A. M. Dimits, T. J. Williams, J. A. Byers, and B. I. Chohen, Phys. Rev. Lett. **77**, 71 (1996).
[8] B. Scot, Phys. Plasmas **7**, 1845 (2000).
[9] T. S. Hahm, K. H. Burrel, Z. Lin, R. Nazikian, and E. J. Synakovskii, Plasma Phys. Controlled Fusion **42**, A205 (2000).
[10] M. Ramisch, U. Stroth, S. Niedner, and B. Scott, New J. Phys. **5**, 12.1 (2003).
[11] P. H. Diamond, S.-I. Itoh, K. Itoh, and T. S. Hahm, to be published in Plasma Phys. Controlled Fusion.
[12] T. S. Hahm, Plasma Phys. Controlled Fusion **44**, A87 (2002).
[13] S. V. Novakovskii, C. S. Liu, R. Z. Sagdeef, and M. N. Rosenbluth, Phys. Plasmas **4**, 4272 (1997).
[14] K. Hallatschek and D. Biskamp, Phys. Rev. Lett. **86**, 1223 (2001).
[15] B. N. Rogers and J. F. Drake, Phys. Rev. Lett. **79**, 229 (1997).
[16] B. N. Rogers, J. F. Drake, and A. Zeiler, Phys. Rev. Lett. **81**, 4396 (1998).
[17] A. B. Hassam and J. F. Drake, Phys. Fluids B **5**, 4022 (1993).
[18] K. Itoh, K. Hallatschek, and S-I. Itoh, Plasma Phys. Controlled Fusion **47**, 451 (2005).
[19] G. R. Mackee, R. J. Fonck, M. Jakubowski, K. H. Burrell, K. Hallastschek, R. A. Moyer, W. Nevins, D. L. Rudakov, and X. Xu, Plasma Phys. Controlled Fusion **45**, A477 (2003).
[20] P. M. Schoch, K. A. Conner, D. R. Demers, and X. Zhang, Rev. Sci. Instrum. **74**, 1846 (2003).
[21] Y. W. Tsui, P. M. Schoch, and A. J. Wootton, Phys. Fluids B **5**, 1274 (1993).
[22] Y. Hamada, A. Nishizawa, T. Ido, T. Watari, M. Kojima, K. Kawasumi, K. Narihara, K. Toi, and JIPP T-IIU Group, Nucl. Fusion **45**, 81 (2005).
[23] Y. Hamada, N. Nishizawa, Y. Kawasumi, A. Fujisawa, H. Iguchi, and JIPP T-IIU Group, Fusion Eng. Des. **34-35**, 663 (1997).
[24] T. Ido, Y. Miura, K. Hoshino, Y. Hamada, Y. Nagashima, H. Ogawa, K. Shinohara, K. Kamiya, A. Nishizawa, Y. Kawasumi, Y. Kusama, and JFT-2M Group, "Electrostatic fluctuation and fluctuation-induced particle flux during formation of the edge transport barrier in the JFT-2M tokamak," in *CD Proceedings of the 20th IAEA Conference on Fusion Energy*, 2004, Portugal, IAEA, EX/4-6Rb.
[25] A. Fujisawa, K. Itoh, H. Iguchi *et al.*, Phys. Rev. Lett. **93**, 165002 (2004).
[26] M. G. Shats and W. M. Solomon, Phys. Rev. Lett. **88**, 045001 (2002).
[27] G. S. Xu, B. N. Wan, M. Song, and J. Li, Phys. Rev. Lett. **91**, 125001 (2003).
[28] G. D. Conway, B. Scott, J. Schirmer, M. Reich, A. Kendl, and ASDEX Upgrade Team, "Direct measurement of zonal flows and geodesic acoustic mode(GAM) oscillations in ASDEX upgrade using doppler reflectometry," in *CD Proceedings of 31st EPS Conference on Controlled Fusion and Plasma Physics*, 2004, European Physical Society, London, paper, P4.124.
[29] T-10 Team, "Transport and turbulence studies in the T-10 tokamak," in *CD Proceedings of the 19th IAEA Conference on Fusion Energy*, 2002, Lyon, IAEA, paper OV/5-2.